Original Article

The factors of fiducial marker motions and individual margin assessment in postoperative breast cancer radiotherapy

Jiaojiao Luo[1], Haiyan Peng[1], Huanli Luo[1], Xiaohua Zeng[2], Fu Jin[1], Yue Xie[1]

[1]Department of Radiation Oncology, Chongqing University Cancer Hospital, Chongqing, China; [2]Department of Breast Cancer, Chongqing University Cancer Hospital, Chongqing, China

Contributions: (I) Conception and design: J Luo, F Jin, Y Xie; (II) Administrative support: F Jin, Y Xie; (III) Provision of study materials or patients: X Zeng; (IV) Collection and assembly of data: H Peng, H Luo, X Zeng, Y Xie; (V) Data analysis and interpretation: All authors; (VI) Manuscript writing: All authors; (VII) Final approval of manuscript: All authors.

Correspondence to: Fu Jin; Yue Xie. Department of Radiation Oncology, Chongqing University Cancer Hospital, 181 Hanyu Road, Shapingba District, Chongqing 400030, China. Email: jfazj@126.com; linmn9@gmail.com.

Background: As a surrogate for the breast tumor bed, individual fiducial markers frequently move during radiotherapy. This study aimed to classify the motions and calculate the individualized target margin.

Methods: The mammary basal diameters (D) and heights (H) were measured to represent breast sizes for 15 patients after breast-conserving surgery. The clinical target volume (CTV) was divided into 4 quadrants by a coordinate system with the center of mass of the tumor bed as the origin. The lateral, anteroposterior, and craniocaudal motions of markers were calculated (M_{LR}, M_{AP}, M_{SI}) based on the difference of the setup errors between the spine matching and the fiducial markers matching. The distances between markers and the innermost, foremost, and uppermost borders of CTV (DS_{LR}, DS_{AP}, DS_{SI}) were recorded.

Results: In the first quadrant, M_{AP} was strongly correlated with D×H ($r>0.80$) when D×H <99.89 cm^2. Both M_{LR} and M_{AP} were positively linearly related to DS_{LR}, DS_{AP}, DS_{SI} ($r>0.85$, $R^2>0.75$). M_{SI} was also positively linearly correlated with DS_{AP} and DS_{LR} ($r>0.90$, $R^2>0.80$). In the fourth quadrant with D×H <90.71 cm^2, only M_{LR} and DS_{LR} showed a linear positive correlation ($r>0.90$, $R^2>0.75$), whereas the others showed linear negative correlations ($r>-0.90$, $R^2>0.80$). The planning target volume (PTV) margin varied significantly between the first and fourth quadrant ($P<0.05$), and the largest margin was 12.4 mm in the craniocaudal direction of the first quadrant with D×H ≥99.89 cm^2.

Conclusions: Fiducial motion is susceptible to breast size and fiducial position, and the individualized PTV margins should take the above factors into account.

Keywords: Breast cancer; fiducial motion; cone-beam CT (CBCT); surgical clip; radiotherapy

Submitted Nov 21, 2022. Accepted for publication Dec 19, 2022.
doi: 10.21037/atm-22-6026
View this article at: https://dx.doi.org/10.21037/atm-22-6026

Introduction

Breast cancer is the most common cancer among women (1). Radiotherapy after breast-conserving surgery has been identified as an effective treatment for early-stage breast cancer (2). Radiation plays very important role in local control of breast cancer following surgery, which can increase the 5-year local control rate by 19% and the 15-year overall survival (OS) rate by 5% (3-5). Accurate location of the target volume after breast-conserving surgery can ensure appropriate radiation while minimizing normal tissue exposure (6,7). However, the breast position and shape are vulnerable to respiratory motion, setup error, and patient immobilization (8,9). This will necessarily lead to a reduction in the precision of radiotherapy. Meanwhile, several studies have shown that surgical clips implanted into the lumpectomy cavity during surgery can improve the accuracy of the irradiated target volume (10-13). Zhang

et al. demonstrated that changes in the center of mass displacement between fiducial markers and the cavity were minimal in all directions and that the fiducial marker is a suitable surrogate for the lumpectomy cavity (14). However, there is significant motion of markers during radiotherapy, especially the inter-fraction motion (15). To ensure that the tumor bed gets enough radiation and avoid excessive exposure for normal tissue, it needs to set appropriate planning target volume (PTV) margins based on fiducial markers motion. Using the fiducial marker as the reference for the tumor bed can effectively reduce the PTV margins, which has been reported in previous study (16). So far, studies about factors that can significantly affect fiducial marker motion are still lacking, and research needs to be conducted to investigate whether there is any correlation between the marker motions and breast position and shape.

The goal of this study was to investigate the clinical factors affecting the fiducial marker motions and to try to define an individualized PTV margin based on these factors. Therefore, the center of mass of the tumor bed was chosen as the origin of a coordinate system in the transverse plane, and the clinical target volume (CTV) was divided into 4 quadrants. The fiducial positions were recorded, and the displacements of each fiducial were calculated in this system. Meanwhile, the mammary basal diameter (D), the mammary height (H), and D×H were used to represent breast size. The correlations among D, H, D×H, and fiducial positions and motions were analyzed. We present the following article in accordance with the MDAR reporting checklist (available at https://atm.amegroups.com/article/view/10.21037/atm-22-6026/rc).

Highlight box

Key findings

- Breast size and fiducial position are significantly correlated with fiducial motions, and the PTV margin should be expanded unevenly based on patient's characteristics.

What is known and what is new?

- The fiducial markers frequently move during radiotherapy. This motion was anisotropic and tended to the right, dorsal and caudal.
- We found out the clinical factors affecting fiducial motion, which provides a reference for the classified management of patients and the individualized PTV margins.

What is the implication, and what should change now?

- Compared with the traditional uniform margin, the individualized PTV margins based on patient's characteristics can further improve the accuracy of radiotherapy.

Methods

Patients

A total of 15 patients who underwent breast-conserving surgery without prosthesis implantation were randomly selected from January to July 2020, including 7 cases of left breast cancer and 8 cases of right breast cancer. All of them had no distant metastasis and the arm movement was not limited. The study was conducted in accordance with the Declaration of Helsinki (as revised in 2013). Individual consent was not required because this was a retrospective study. The study was approved by the ethics committee of Chongqing University Cancer Hospital (No. CZLS2022221-A).

All patients were immobilized using a thermoplastic mask in the supine position. Both arms were raised above the head. A computed tomography (CT) scan was performed in the treatment position with a 2-mm slice thickness on a Brilliance-16 system (Philips Medical Systems, Inc., Cleveland, OH, USA). Target delineation was carried out in the Eclipse treatment planning system (Varian Medical Systems, Milpitas, CA, USA). All patients received whole breast irradiation (WBI) at a total of 50 Gy in 25 fractions. Cone-beam CT (CBCT) was performed twice a week, and CBCT images were registered to the planning CT images to calculate the position shifts.

Fiducial placement

A total of 5 fiducial markers were placed at the margins of the lumpectomy cavity in 15 patients who underwent a lumpectomy, and the standard surgical procedure was a closed-cavity technique. The length of a fiducial marker is 2 mm.

Statistical analysis

We defined the tangent through the top of the pectoralis major arc as D, and the vertical line of D across the highest point of the breast was defined as H (as shown in *Figure 1*). In the previous study, we found that D, H, and D×H were all significantly correlated to breast size (r=0.62, 0.81, and 0.83, respectively), and the correlation was the largest in the middle of the breast. Thus, we chose to measure D and H at the tracheal bifurcation. D, H, and D×H were used to

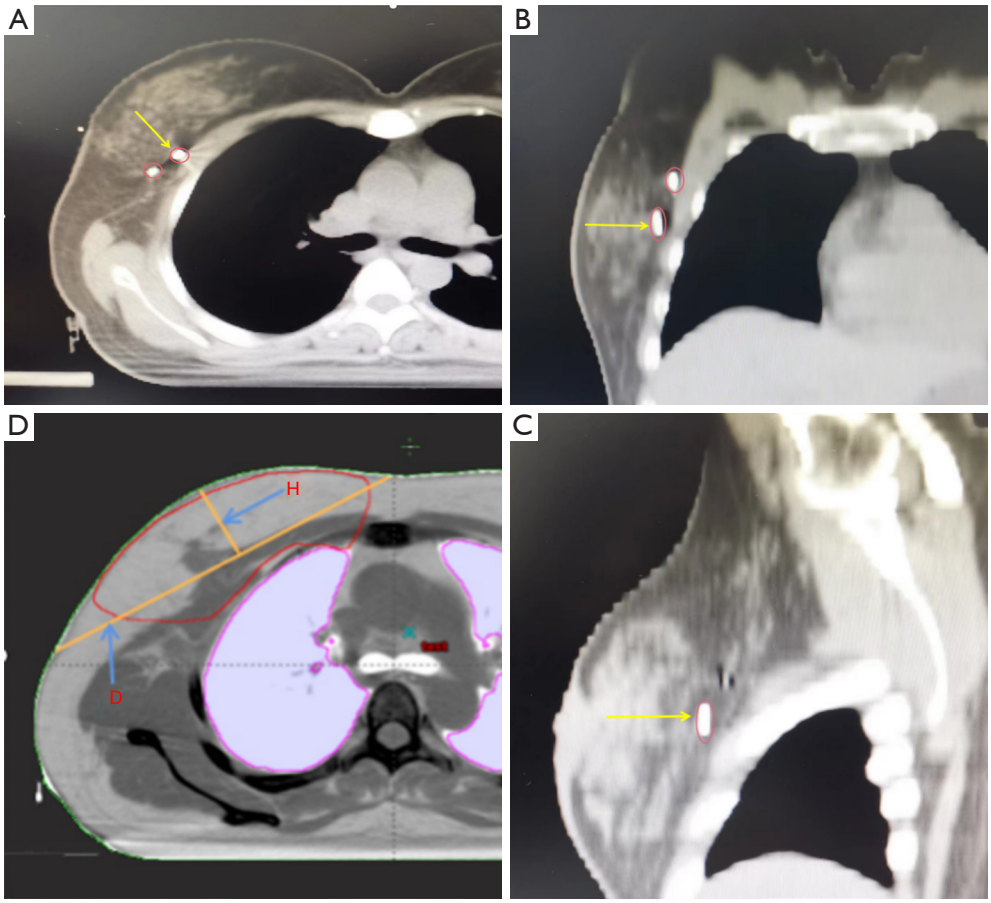

Figure 1 Sectional display of intraoperative implanted surgical clip. (A-C) The yellow arrow points to a surgical clip in the transverse, coronal, and sagittal view, respectively. (D) The definitions of mammary basal diameter [D] and mammary height axis [H].

classify breast size (17). Correspondingly, m_D, m_H, and $m_{D\times H}$ were used to represent their medians.

In the Eclipse treatment planning system, we get the tumor bed centroid. In the axial plane where the mass center of the tumor bed is located, we took the mass center of the tumor bed as a coordinate origin to divide the CTV into 4 quadrants, and relocated the fiducial markers to different quadrants. As described below, the first quadrant was close to midsternal line and located on the upper side of the origin; the second quadrant was far away from midsternal line and located on the upper side of the origin; the third quadrant was far away from midsternal line and located on the downside of the origin; the fourth quadrant was close to midsternal line and located on the downside of the origin. We moved the auxiliary line to the innermost, foremost, and uppermost side of the CTV, and the corresponding coordinates were sequentially recorded as (x_0, y_0, z_0). Then, we moved the auxiliary line to the center of fiducial markers, and the coordinates were recorded as (x_1, y_1, z_1). Additionally, (x_1-x_0, y_1-y_0, z_1-z_0) indicated the distance from fiducials to the innermost, foremost, and uppermost sides of the CTV. They were recorded as DS_{LR}, DS_{AP}, and DS_{SI}, which stands for lateral, anteroposterior, and craniocaudal distance, respectively.

We assessed setup errors using the following 2 methods: (I) matching the spine close to the target; (II) matching the fiducial markers. The errors using the first method were from the routine position shifts and the errors using the second method included the uncertainties from respiratory motion and position shifts. The difference between 2 kinds of setup errors was the fiducial marker motion induced only by respiratory motion. They were recorded as M_{LR}, M_{AP}, and M_{SI}, which stands for lateral, anteroposterior, and craniocaudal motion, respectively. The three-dimensional movement (M_{3D}) of each fiducial marker was calculated using the following formula (18):

Table 1 General clinical data of 15 patients enrolled

The serial number	Times[a] (weeks)	Times[b] (days)	Operation methods	Axillary lymph node*
1	24	6	Lumpectomy	Sentinel lymph node biopsy
2	25	3	Lumpectomy	Sentinel lymph node biopsy
3	25	5	Lumpectomy	Sentinel lymph node biopsy
4	23	2	Lumpectomy	Sentinel lymph node biopsy
5	24	4	Lumpectomy	Sentinel lymph node biopsy
6	15	5	Lumpectomy	Sentinel lymph node biopsy
7	14	4	Lumpectomy	Sentinel lymph node biopsy
8	26	2	Lumpectomy	Sentinel lymph node biopsy
9	24	5	Lumpectomy	Sentinel lymph node biopsy
10	20	1	Lumpectomy	Sentinel lymph node biopsy
11	20	6	Lumpectomy	Sentinel lymph node biopsy
12	25	5	Lumpectomy	Sentinel lymph node biopsy
13	25	1	Lumpectomy	Sentinel lymph node biopsy
14	26	4	Lumpectomy	Sentinel lymph node biopsy
15	33	5	Lumpectomy	Sentinel lymph node biopsy

[a], refers to the time interval between surgery and initial radiotherapy; [b], refers to the time interval between simulation and initial radiotherapy; *, refers to the method of axillary lymph node management.

$$M_{3D} = \sqrt{M_{LR}^2 + M_{AP}^2 + M_{SI}^2} \quad [1]$$

We used SPSS 20.0 (IBM Corp., Armonk, NY, USA) and Origin 9.0 (OriginLab, Northampton, MA, USA) to analyze the correlation between M_{LR}, M_{AP}, M_{SI}, M_{3D} and D, H, D×H, DS_{LR}, DS_{AP}, DS_{SI}, expecting to find the factors influencing the fiducial marker motion. Then, we calculated the PTV margin using the van Herk margin recipe, which provided a margin for adequate treatment in 90% of the patients (19).

Results

A total of 15 patients, all female, were included in this study. Their ages ranged from 23 to 56 years with an average of 43 years. The mammary basal diameter (D) ranged from 17.32 to 22.53 cm with a mean of 19.72 cm, and the mammary height axis (H) ranged from 3.58 to 6.82 cm with a mean of 4.79 cm. The D×H ranged from 66.69 to 148.70 cm^2 with a mean of 95.29 cm^2. Other relevant information about patients is shown in *Table 1*.

The fiducial motions

Our study analyzed 372 fractions of clinical data from 39 fiducial markers (including 19 in the first quadrant, 6 in the second quadrant, 3 in the third quadrant and 11 in the fourth quadrant). The distributions of the displacements of all single fiducials are shown in *Figure 2*. It showed the 1-dimensional displacements of each fiducial and the combined 3-dimensional displacements of each fiducial. It could be modelled as a Gaussian process. M_{LR}, M_{AP}, M_{SI}, and M_{3D} were shown as follows (average ± standard deviation): 2.2±3.0, −1.1±3.6, 0.8±4.7, 6.5±2.7 mm. According to the Gaussian model, the 1-dimensional displacements was concentrated in the range of −5 to 5 mm, in which M_{LR} accounted for 81.6%, M_{AP} was 81.5%, and M_{SI} was 70.4%. The fiducial migration was anisotropic, and tended to the right, dorsal, and caudal.

Correlation with breast size

Due to limited samples located in the second and third

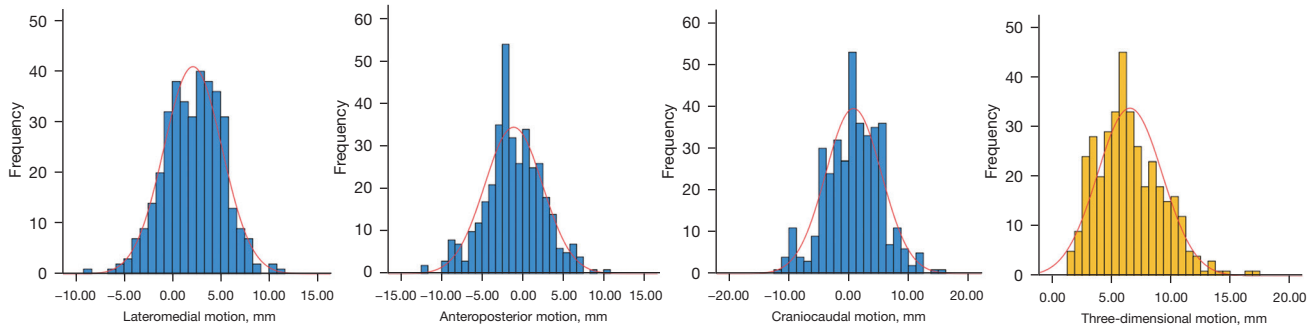

Figure 2 Histograms of fiducial motions. Positive values for the 1-dimensional displacements indicate motions in the right, ventral, and caudal direction.

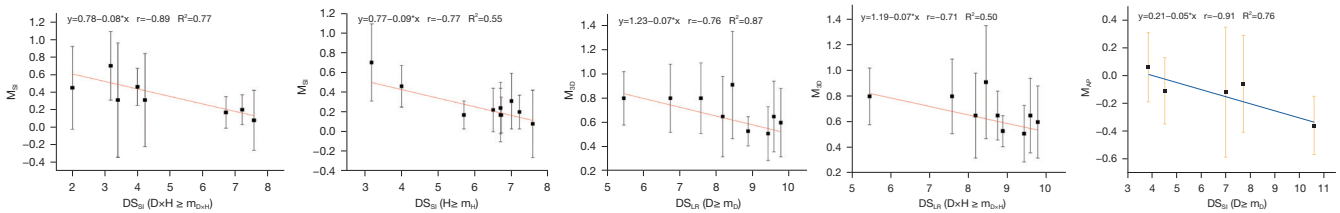

Figure 3 Linear fit plots between the fiducial motion and fiducial position of patients with larger breasts. The first quadrant is marked with a red line and the fourth quadrant with a blue line. In the first quadrant, m_D =19.53 cm, m_H =4.98 cm, $m_{D\times H}$ =99.89 cm^2; in the fourth quadrant, m_D =19.41 cm, m_H =4.41 cm, $m_{D\times H}$ =90.71 cm^2. m, median; D, the mammary basal diameter; H, the mammary height axis.

quadrants in this study, these markers were not included in the analysis. Our study only analyzed the markers in the first and fourth quadrants, and did not exclude any data points. When $D < m_D$ and $D\times H < m_{D\times H}$, M_{LR}, M_{AP}, and M_{SI} all had a statistically significant but weak correlation with D and D×H ($P<0.05$) both in the first and fourth quadrants, except for M_{AP} located in the first quadrant, which was significantly positively correlated with D, H, and D×H (r=0.517, 0.691, and 0.805, respectively). For M_{3D}, there was no correlation with D, H, and D×H in the first quadrant, however it had a negatively weak correlation with H and D×H in the fourth quadrant only when $H \geq m_H$ and $D\times H \geq m_{D\times H}$, and the Pearson correlation coefficient r was −0.353 and −0.312 ($P<0.05$).

Correlation with fiducial position

The linear fitting diagrams when $D \geq m_D$, $H \geq m_H$, and $D\times H \geq m_{D\times H}$ are shown in *Figure 3*. In the first quadrant, M_{SI} showed a strong linear negative correlation with DS_{SI} both in H and D×H classifications [r (R^2) =−0.77 (0.55) *vs.* −0.89 (0.77)]. M_{3D}, was strongly linearly negatively correlated with DS_{LR} in D and D×H classifications [r (R^2) =−0.76 (0.87) *vs.* −0.71 (0.50)]. In the fourth quadrant, only under the D classification, M_{AP} and DS_{SI} showed a strong linear negative correlation [r (R^2) =−0.91 (0.76)].

The linear fitting diagrams when $D<m_D$, $H<m_H$, $D\times H<m_{D\times H}$ are shown in *Figure 4* (only showing the most representative groups, and the others are shown in *Table 2*). It can be seen that under D and D×H classifications, M_{LR} and M_{AP} located in the first quadrant all had a strong linear positive correlation with DS_{LR}, DS_{AP} and DS_{SI} (r>0.8). In the D×H classification the r (R^2) values of M_{LR} and DS_{LR}, DS_{AP} were all greater than that in the D classification [r (R^2) =0.94 (0.87), 0.94 (0.86) *vs.* 0.88 (0.74), 0.88 (0.75)], which was the same as M_{AP} and DS_{LR}, DS_{AP} [r (R^2) =0.87 (0.76), 0.91 (0.80) *vs.* 0.83 (0.64), 0.84 (0.67)]. For M_{SI}, whether it was D, H, or D×H classification, M_{SI}, DS_{LR}, and DS_{AP} all showed a significant linear positive correlation [r (R^2) =0.77 (0.53), 0.82 (0.62) *vs.* 0.86 (0.68), 0.88 (0.74) *vs.* 0.91 (0.80), 0.94 (0.87)]. The 1-dimensional displacements of fiducials located in the fourth quadrant were correlated with the fiducial position only in the H and D×H classifications. As explained below: M_{AP} and DS_{LR}, M_{SI} and DS_{AP} all showed

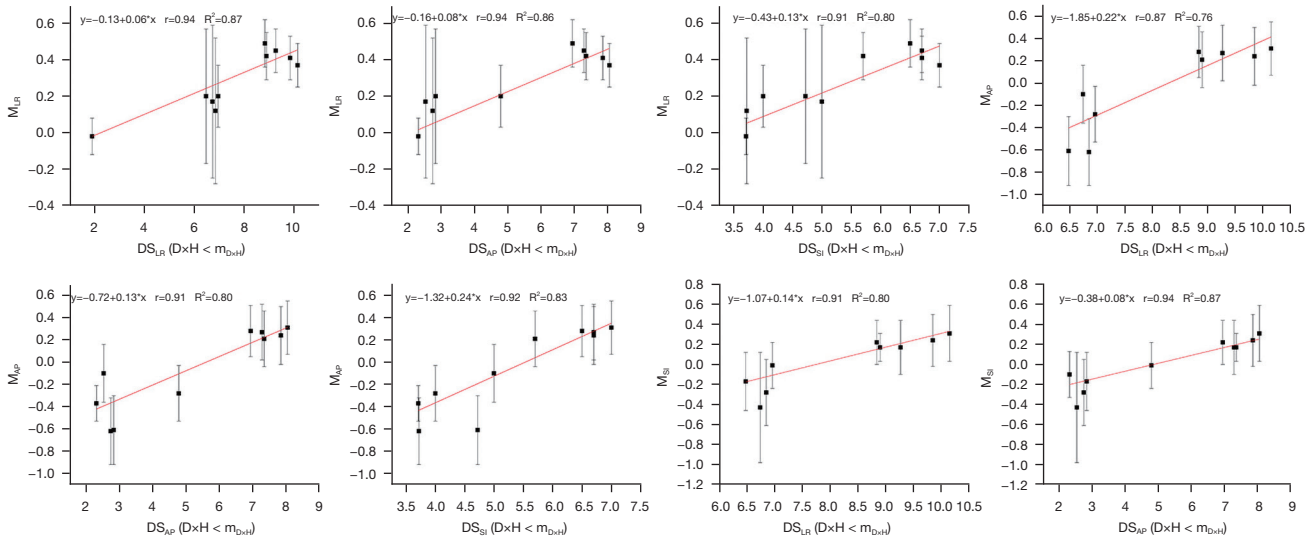

Figure 4 Linear fitting plots between the fiducial motion and fiducial position of patients with small breasts (in the first quadrant); m_D =19.53 cm, m_H =4.98 cm, $m_{D\times H}$ =99.89 cm^2. m, median; D, the mammary basal diameter; H, the mammary height axis.

a strong linear negative correlation, the corresponding r (R^2) values were −0.96 (0.91) and −0.95 (0.87) both in H and D×H classification. However M_{LR} was strongly linearly positively correlated with DS_{LR}, and the r (R^2) value was 0.91 (0.77). For M_{3D}, it was significantly linearly positively correlated with DS_{LR} in 3 classifications, and the r (R^2) values are 0.74 (0.54), 0.89 (0.71), and 0.89 (0.71).

The correlation coefficient (r) and linear goodness of fit (R^2) between fiducial motion and the fiducial position are shown in *Table 2*. The D×H classification (R^2>0.7) was generally better than the D (R^2>0.6) and H classification (R^2>0.5).

The individualized PTV margins

We calculated the PTV margin according to the van Herk (19) margin formula 2.5Σ+0.7σ. We can get details from *Table 3*. In the first quadrant, when D×H <99.89 cm^2, the margin in the left, right, cranial, and caudal directions were 0.63, 0.73, 0.93, and 0.64 (cm) in turn, which was statistically significantly different from that when D×H ≥99.89 cm^2 (P<0.05), and when D×H ≥99.89 cm^2, the corresponding margins were 0.69, 1.01, 1.05, and 1.24 (cm). In the fourth quadrant, because of the small sample size, the margins had no statistical difference between the D×H <90.71 cm^2 and the D×H ≥90.71 cm^2 classifications, but it showed a smaller margin than that in the first quadrant. The PTV margins in the ventral, dorsal, cranial, and caudal directions had a statistically significant difference between the first and fourth quadrants (P<0.05).

Discussion

This study divided the CTV into 4 quadrants, and used D, H, and D×H to classify the breast size for the first time. We analyzed fiducial marker motions and its correlation with clinical factors under the same classification of breast size and quadrant position, and we found that the fiducial marker motion is easily affected by breast size and the distance from fiducials to the edge of CTV, especially the 1-dimensional movements in the first quadrant.

We calculated the average and standard deviation of each fiducial motion during the whole treatment process, and fitted it with fiducial position as shown in *Figure 3* and *Figure 4*. When D×H < $m_{D\times H}$, for M_{LR}, there was a strong linear positive correlation with DS_{LR} both in the first and fourth quadrants, but for M_{AP} and M_{SI}, there was a linear negative correlation with fiducial position in the fourth quadrant, whereas there was a linear positive correlation with fiducial position in the first quadrant. Maybe the reason is that the first and fourth quadrants are all located in the medial side of the tumor bed centroid. When D×H ≥ $m_{D\times H}$, the correlation between the fiducial motion and the fiducial position is weaker than that in D×H < $m_{D\times H}$. The reason is that in patients with larger breast, the breast shape changes greatly (20), and the gravity will have a greater

Table 2 Linear fits between the fiducial motion and the fiducial position (R^2/r values)

Quadrant	Motion	D			H			D×H		
		DS_{LR}	DS_{AP}	DS_{SI}	DS_{LR}	DS_{AP}	DS_{SI}	DS_{LR}	DS_{AP}	DS_{SI}
First	M_{3D}	0.87/–0.76*	–	–	–	–	–	0.50/–0.71*	–	–
	M_{LR}	0.74/0.88	0.75/0.88	0.82/0.91	–	–	–	0.87/0.94	0.86/0.94	0.80/0.91
	M_{AP}	0.64/0.83	0.67/0.84	0.84/0.93	–	0.59/0.81	–	0.76/0.87	0.80/0.91	0.83/0.92
	M_{SI}	0.53/0.77	0.62/0.82	–	0.68/0.86	0.74/0.88	0.55/–0.77*	0.80/0.91	0.87/0.94	0.77/–0.89*
Fourth	M_{3D}	0.54/0.74	–	–	0.71/0.89	–	–	0.71/0.89	–	–
	M_{LR}	–	–	–	0.77/0.91	–	–	0.77/0.91	–	–
	M_{AP}	–	–	0.76/–0.91*	0.91/–0.96	–	–	0.91/–0.96	–	–
	M_{SI}	–	–	–	–	0.87/–0.95	–	–	0.87/–0.95	–

*, indicated the linear fits of patients with the larger breast (D≥ mD, H≥ mH, D×H ≥ mD×H). m, median; D, the mammary basal diameter; H, the mammary height axis; DS_{LR}, the lateral distance from fiducials to the innermost border of the clinical target volume; DS_{AP}, the anteroposterior distance from fiducials to the foremost border of the clinical target volume; DS_{SI}, the craniocaudal distance from fiducials to the uppermost border of the clinical target volume; M_{3D}, the three-dimensional movement; M_{LR}, the lateral motions; M_{AP}, the anteroposterior motions; M_{SI}, the craniocaudal motions.

Table 3 PTV margins based on different breast size and quadrant position of lesion. The positive signals in the LR, AP and SI directions indicate the right, ventral and caudal direction in turn, and the negative signals mean the opposite directions

Quadrant	Direction	D (cm)		H (cm)		D×H (cm^2)	
		D< m_D	D≥ m_D	H< m_H	H≥ m_H	D×H < $m_{D×H}$	D×H ≥ $m_{D×H}$
First	$LR_{(+/-)}$	0.71/0.64	1.04/0.69	0.69/0.56	0.89/0.77	0.73/0.63	1.01/0.69
	$AP_{(+/-)}$	0.65/1.02	0.63/0.82	0.40/1.05	0.69/0.81	0.68/1.06	0.64/0.81
	$SI_{(+/-)}$	0.73/0.65	1.29/1.21	1.29/0.96	0.97/0.99	0.64/0.93	1.24/1.05
Fourth	$LR_{(+/-)}$	0.68/0.46	0.91/0.38	0.75/0.40	0.83/0.49	0.76/0.39	0.80/0.46
	$AP_{(+/-)}$	0.23/0.73	0.82/0.63	0.62/0.71	0.90/0.70	0.66/0.73	0.82/0.68
	$SI_{(+/-)}$	0.73/0.99	1.26/1.11	1.05/1.08	0.89/0.26	0.70/1.11	1.02/0.50

PTV, planning target volume; LR, left-right; AP, anterior-posterior; SI, superior-inferior; D, the mammary basal diameter; H, the mammary height axis; m, median.

dispersion effect on the displacement of the breast (21), which increase the uncertainty of fiducial motions.

Hoekstra thought that the motion of fiducials relative to the tumor bed between planning CT and treatment was clinically significant (15), whereas the fiducial offset was mainly composed of inter-fraction motion, and the intra-fractional motion was very small (9). We found that the fiducial motion tended to the dorsal and caudal, which was basically the same as in previous studies (11,22,23), and the magnitude of fiducial motion depended on patients' characteristics and tumor cavity location (23). Therefore, we classified fiducials according to patients' characteristics and fiducial position, and calculated corresponding fiducial motion and PTV margins. The maximum margin was 12.4 mm, occurring in the craniocaudal direction, which was greater than 10.2 mm in Harris *et al.* study (24). Harris used 2-dimensional imaging technology, which was limited by the fiducial visibility, it would underestimate the fiducial motion compared with the CBCT imaging technology in this study. Furthermore, in this study, patients were immobilized using a body board and thermoplastic mask, which was different from Harris *et al.* study (24). The setup errors would change greatly when using different patient positioning devices (15). We found that breast size

and fiducial position could influence fiducial motion, and the corresponding PTV margins also had a statistically significant difference, but the individualized PTV margin still needs to be verified with a larger sample size.

In addition, if the time interval between surgery and radiotherapy was short, postoperative seroma, fibrosis, contraction, and fluid absorption would lead to changes in the size and shape of the resection cavity and affect the fiducial motion (22,25). The seroma basically disappeared 14 weeks after the operation (26). In this study, all patients received radiotherapy at least 14 weeks after surgery. Since the time interval between simulation and treatment could affect the fiducial motion (15), in our study, the treatment occurred within a week after simulation.

Implantation of fiducial markers in breast conserving surgery is widely used in clinical practice to improve the accuracy of target location and 4 or more fiducials are necessary (12). All fiducial markers are titanium clips, which have a good biocompatibility and are safe for patients. In our study, although 5 fiducials were implanted evenly in each patient during the surgical suturing process, the fiducials would inevitably approach one another or fuse together, which would increase the differences between fiducials. Furthermore, the fiducials enrolled were more concentrated on the inner side of the centroid, so we focused on the analysis of the mobility and influencing factors of fiducials in the first and fourth quadrants. To attain a more accurate rule, the fiducials were classified based on the breast size and quadrant position, which also resulted in fewer data points in the fourth quadrant. This problem also existed in the calculation of PTV margins. However, the research showed that there was an obvious linear correlation trend between the mobility and the position of fiducials in the first and fourth quadrants. Therefore, in the next study, we will supplement patients with fiducials in the second and third quadrants and increase the number of samples for further validation.

Conclusions

Our study showed that the fiducial motion tended to the right, dorsal, and caudal directions. Both the breast size (D×H) and the distance from fiducial markers to the edge of CTV could influence the 1-dimensional motions of fiducials, and the maximum margin was 12.4 mm appearing in the craniocaudal direction of the first quadrant with the D×H ≥99.89 cm^2. It suggested that patients should be classified to manage and individualized PTV margins should be calculated according to the breast size and the location of the lesion in breast cancer radiotherapy.

Acknowledgments

The authors thank the following colleagues for their assistance and advice in this study: Han Yang, Shi Li, Guang Li, Xian Zhou, and Zhengwen Shen from the department of Radiation Oncology, Chongqing University Cancer Hospital.

Funding: This work was partially supported by Chongqing Medical Scientific Research Project (Joint Project of Chongqing Health Commission and Science and Technology Bureau) under Grant No. 2022DBXM005.

Footnote

Reporting Checklist: The authors have completed the MDAR reporting checklist. Available at https://atm.amegroups.com/article/view/10.21037/atm-22-6026/rc

Data Sharing Statement: Available at https://atm.amegroups.com/article/view/10.21037/atm-22-6026/dss

Conflicts of Interest: All authors have completed the ICMJE uniform disclosure form (available at https://atm.amegroups.com/article/view/10.21037/atm-22-6026/coif). The authors have no conflicts of interest to declare.

Ethical Statement: The authors are accountable for all aspects of the work in ensuring that questions related to the accuracy or integrity of any part of the work are appropriately investigated and resolved. The study was conducted in accordance with the Declaration of Helsinki (as revised in 2013). Individual consent was not required because this was a retrospective study. The study was approved by the ethics committee of Chongqing University Cancer Hospital (No. CZLS2022221-A).

References

1. Łukasiewicz S, Czeczelewski M, Forma A, et al. Breast Cancer-Epidemiology, Risk Factors, Classification, Prognostic Markers, and Current Treatment Strategies-An Updated Review. Cancers (Basel) 2021.
2. Tutzauer J, Sjöström M, Holmberg E, et al. Breast cancer hypoxia in relation to prognosis and benefit from radiotherapy after breast-conserving surgery in a large, randomised trial with long-term follow-up. Br J Cancer 2022;126:1145-56.
3. Sharma SC, Kapoor R. Role of Radiotherapy in Breast Cancer. In: Sharma SC, Mazumdar A, Kaushik R. editors. Breast Cancer. Springer, Singapore; 2022.
4. Wei X, Liu M, Ding Y, et al. Setup errors and effectiveness of Optical Laser 3D Surface imaging system (Sentinel) in postoperative radiotherapy of breast cancer. Sci Rep 2018;8:7270.
5. Marks LB, Gupta GP, Muss HB, et al. Mastectomy May Be an Inferior Oncologic Approach Compared to Breast Preservation. Int J Radiat Oncol Biol Phys 2019;103:78-80.
6. Kaufman CS, Cross MJ, Barone JL, et al. A Three-Dimensional Bioabsorbable Tissue Marker for Volume Replacement and Radiation Planning: A Multicenter Study of Surgical and Patient-Reported Outcomes for 818 Patients with Breast Cancer. Ann Surg Oncol 2021;28:2529-42.
7. Feng CH, Gerry E, Chmura SJ, et al. An image-guided study of setup reproducibility of postmastectomy breast cancer patients treated with inverse-planned intensity modulated radiation therapy. Int J Radiat Oncol Biol Phys 2015;91:58-64.
8. van der Salm A, Murrer L, Steenbakkers I, et al. Actual target coverage after setup verification using surgical clips compared with external skin markers in postoperative breast cancer radiation therapy. Pract Radiat Oncol 2017;7:e369-76.
9. Hattel SH, Andersen PA, Wahlstedt IH, et al. Evaluation of setup and intrafraction motion for surface guided whole-breast cancer radiotherapy. J Appl Clin Med Phys 2019;20:39-44.
10. Ding Y, Li J, Wang W, et al. A comparative study on the volume and localization of the internal gross target volume defined using the seroma and surgical clips based on 4DCT scan for external-beam partial breast irradiation after breast conserving surgery. Radiat Oncol 2014;9:76.
11. Yue NJ, Goyal S, Kim LH, et al. Patterns of intrafractional motion and uncertainties of treatment setup reference systems in accelerated partial breast irradiation for right- and left-sided breast cancer. Pract Radiat Oncol 2014;4:6-12.
12. Lee PY, Lin CY, Chen SW, et al. A topology-based method to mitigate the dosimetric uncertainty caused by the positional variation of the boost volume in breast conservative radiotherapy. Radiat Oncol 2017;12:55.
13. Sung S, Lee JH, Lee JH, et al. Displacement of Surgical Clips during Postoperative Radiotherapy in Breast Cancer Patients Who Received Breast-Conserving Surgery. J Breast Cancer 2016;19:417-22.
14. Zhang Y, Mutter RW, Park SS, et al. Carbon Fiducial Image Guidance Increases the Accuracy of Lumpectomy Cavity Localization in Radiation Therapy for Breast Cancer. Pract Radiat Oncol 2019;9:e14-21.
15. Hoekstra N, Habraken S, Swaak-Kragten A, et al. Fiducial marker motion relative to the tumor bed has a significant impact on PTV margins in partial breast irradiation. Radiother Oncol 2021;163:1-6.
16. Park CK, Pritz J, Zhang GG, et al. Validating fiducial markers for image-guided radiation therapy for accelerated partial breast irradiation in early-stage breast cancer. Int J Radiat Oncol Biol Phys 2012;82:e425-e431.
17. Lim LY, Ho PJ, Liu J, et al. Determinants of breast size in Asian women. Sci Rep 2018;8:1201.
18. Hwang JM, Hung JY, Tseng YH, et al. Use of electronic portal images to evaluate setup error and intra-fraction motion during free-breathing breast IMRT treatment. Med Dosim 2019;44:233-8.
19. van Herk M. Errors and margins in radiotherapy. Semin Radiat Oncol 2004;14:52-64.
20. Seppälä J, Vuolukka K, Virén T, et al. Breast deformation during the course of radiotherapy: The need for an additional outer margin. Phys Med 2019;65:1-5.
21. Wang W, Li JB, Hu HG, et al. Correlation between target motion and the dosimetric variance of breast and organ at risk during whole breast radiotherapy using 4DCT. Radiat Oncol 2013;8:111.
22. Hirata K, Yoshimura M, Mukumoto N, et al. Three-dimensional intrafractional internal target motions in accelerated partial breast irradiation using three-dimensional conformal external beam radiotherapy. Radiother Oncol 2017;124:118-23.
23. Reitz D, Carl G, Schönecker S, et al. Real-time intra-fraction motion management in breast cancer

radiotherapy: analysis of 2028 treatment sessions. Radiat Oncol 2018;13:128.
24. Harris EJ, Donovan EM, Coles CE, et al. How does imaging frequency and soft tissue motion affect the PTV margin size in partial breast and boost radiotherapy? Radiother Oncol 2012;103:166-71.
25. Harris EJ, Mukesh MB, Donovan EM, et al. A multicentre study of the evidence for customized margins in photon breast boost radiotherapy. Br J Radiol 2016;89:20150603.
26. Kader HA, Truong PT, Pai R, et al. When is CT-based postoperative seroma most useful to plan partial breast radiotherapy? Evaluation of clinical factors affecting seroma volume and clarity. Int J Radiat Oncol Biol Phys 2008;72:1064-9.

(English Language Editor: J. Jones)

Cite this article as: Luo J, Peng H, Luo H, Zeng X, Jin F, Xie Y. The factors of fiducial marker motions and individual margin assessment in postoperative breast cancer radiotherapy. Ann Transl Med 2022;10(24):1359. doi: 10.21037/atm-22-6026

